

Formation and growth of atmospheric nanoparticles in the eastern Mediterranean: Results from long-term measurements and process simulations

Nikos Kalivitis^{1,2}, Veli-Matti Kerminen³, Giorgos Kouvarakis¹, Iasonas Stavroulas^{1,4}, Evaggelia Tzitzikalaki¹, Panayiotis Kalkavouras^{1,5}, Nikolaos Daskalakis^{1,6}, Stelios Myriokefalitakis^{5,7}, Aikaterini Bougiatioti⁵, Hanna Elina Manninen⁸, Pontus Roldin⁹, Tuukka Petäjä³, Michael Boy³, Markku Kulmala³, Maria Kanakidou¹, and Nikolaos Mihalopoulos^{1,5}

1. Environmental Chemical Processes Laboratory, Chemistry Department, University of Crete, 70013, Heraklion, Greece

2. Institute for Astronomy, Astrophysics, Space Applications and Remote Sensing, National Observatory of Athens, I. Metaxa & Vas. Pavlou, 15236 Palea Penteli, Greece

3. Institute for Atmospheric and Earth System Research, Gustaf Hållströmin katu 2, P.O. Box 64, FI-00014 University of Helsinki

4. Energy, Environment and Water Research Center, The Cyprus Institute, Nicosia 2121, Cyprus

5. Institute for Environmental Research & Sustainable Development, National Observatory of Athens, I. Metaxa & Vas. Pavlou, 15236 Palea Penteli, Greece

6. Laboratory for Modeling and Observation of the Earth System (LAMOS), Institute of Environmental Physics (IUP), University of Bremen, Bremen, Germany,

7. Institute for Marine and Atmospheric Research (IMAU): Utrecht, Netherlands

8. Experimental Physics Department, CERN, 1211 Geneva, Switzerland

9. Lund University

Correspondence to: N. Kalivitis (nkativitis@uoc.gr) and N. Mihalopoulos (nmihalo@noa.gr)

1 Abstract

2 Atmospheric New Particle Formation (NPF) is a common phenomenon all over the world. In
3 this study we present the longest time series of NPF records in the eastern Mediterranean
4 region by analyzing ten years of aerosol number size distribution data obtained with a mobility
5 particle sizer. The measurements were performed at the Finokalia environmental research
6 station on Crete, Greece during the period June 2008-June 2018. We found that NPF took
7 place 27% of the available days, undefined days were 23% and non-event days 50%. NPF is
8 more frequent in April and May probably due to the terrestrial biogenic activity and is less
9 frequent in August. Throughout the period under study, nucleation was observed also during
10 the night. Nucleation mode particles had the highest concentration in winter and early spring,
11 mainly because of the minimum sinks, and their average contribution to the total particle
12 number concentration was 8%. Nucleation mode particle concentrations were low outside
13 periods of active NPF and growth, so there are hardly any other local sources of sub-25 nm
14 particles. Additional atmospheric ion size distribution data simultaneously collected for more
15 than two years period were also analyzed. Classification of NPF events based on ion
16 spectrometer measurements differed from the corresponding classification based on a
17 mobility spectrometer, possibly indicating a different representation of local and regional NPF
18 events between these two measurement data sets. We used MALTE-box model for a
19 simulation case study of NPF in the eastern Mediterranean region. Monoterpenes
20 contributing to NPF can explain a large fraction of the observed NPF events according to our
21 model simulations. However the parametrization that resulted after sensitivity tests was
22 significantly different from the one applied for the boreal environment.

23 1) Introduction

24 Most of the atmospheric aerosol particles, and a substantial fraction of particles able to act as
25 cloud condensation nuclei (CCN), have been estimated to originate from new particle
26 formation (NPF) taking place in the atmosphere (Spracklen et al. 2006; Kerminen et al., 2012;
27 Gordon et al., 2017). The exact mechanisms driving atmospheric NPF and subsequent particle
28 growth processes are still not fully understood, nor are the roles of different vapors and ions
29 in these processes (Kulmala et al., 2014; Lehtipalo et al., 2016; Tröstl et al., 2016). In order to
30 understand how aerosol particles affect regional and global climate and air quality, it is
31 necessary to quantify the factors that determine the occurrence of NPF and characterize the
32 parameters that describe the strength of NPF, such as the new particle formation and growth
33 rates, in various environments.

1 While NPF has been reported to take place worldwide (Kulmala et al., 2004a; Wang et al.,
2 2017), observational studies on this subject are scarce in rural sub-tropical environments. It
3 has been shown that the processes responsible for particle formation and growth differ
4 substantially across the European continent (Dall'Osto et al., 2018).

5 Several studies have investigated NPF in eastern Mediterranean and found it to be a frequent
6 phenomenon. Lazaridis et al. (2006) first reported NPF at the area and correlated these events
7 to polluted air masses. Petäjä et al. (2007) presented NPF in Athens metropolitan area and
8 showed that under the influence of urban pollution, condensing species leading to growth of
9 the new particles are far more hygroscopic than under cleaner conditions. NPF events have
10 also been reported to be frequent at the urban environment of Thessaloniki (Siakavaras et al.,
11 2016). Kalivitis et al. (2008) showed that precursors and nucleation mode particles experience
12 strong scavenging on Crete island during summer. Pikridas et al. (2012) suggested that
13 nucleation events occurred only when accumulation mode particles were neutral, being
14 consistent with the hypothesis that a lack of NH_3 , during periods when particles are acidic,
15 may limit nucleation in sulfate-rich environments such as the eastern Mediterranean.
16 Additionally, based on ion observations, Pikridas et al. (2012) showed that NPF is more
17 frequent in winter. By using the same data set from eastern Mediterranean, Kalivitis et al.
18 (2012) reported night-time enhancements in ion concentrations with a plausible association
19 with NPF, being among the very few locations where such observations have been made.
20 Manninen et al. (2010) presented an analysis of a full year of observations of NPF with
21 atmospheric ion spectrometers at various locations across Europe during the EUCAARI project
22 and showed that NPF is less frequent in the eastern Mediterranean site than in other, mostly
23 continental, European sites. On the other hand, Berland et al. (2017) showed that similar
24 patterns are being observed throughout the Mediterranean when comparing observations
25 from the island of Crete to a western Mediterranean site in terms of the frequency of
26 occurrence, seasonality, and particle formation and growth rates. Kalivitis et al. (2015) studied
27 for the first time the NPF-CCN link using observations of particle number size distributions,
28 CCN and high-resolution aerosol chemical composition for the eastern Mediterranean
29 atmosphere. From the hygroscopicity of the particles in different size fractions, it was
30 concluded that smaller particles during active NPF periods tend to be less hygroscopic (and
31 richer in organics) than larger ones. Finally, Kalkavouras et al. (2017) reported that NPF may
32 result in higher CCN number concentrations, but the effect on cloud droplet number is limited
33 by the prevailing meteorology.

In this work, we present results from the analysis of ten years of aerosol particles number size distributions and more than two years of atmospheric ion size distributions, representing the longest published NPF data set in the Mediterranean atmosphere. The main questions we wanted to address were: 1) How often does NPF take place in eastern Mediterranean, what are the characteristics of this phenomenon and to what extent has it changed over the period under study? 2) Are there features in NPF observed at the study area that are not common in other locations? and 3) How well can numerical models, used in different environmental conditions, represent NPF in this subtropical environment?

2) Materials and methods

2.1) Measurements

Measurements presented in this work were carried out at the atmospheric observation station of the University of Crete at Finokalia, Crete, Greece (35°20'N, 25°40'E, 250m a.s.l.) over ten years, between June 2008 and June 2018. The Finokalia station (<http://finokalia.chemistry.uoc.gr/>) is a European supersite for aerosol research, part of the ACTRIS (Aerosols, Clouds, and Trace gases Research Infrastructure) Network. The station is located at the top of a hill over the coastline, in the north east part of the island of Crete (Mihalopoulos et al., 1997). The station is representative for the marine background conditions of eastern Mediterranean (Lelieveld et al., 2002), with negligible influence by local anthropogenic sources. The nearest major urban center in the area is Heraklion with approximately 200 000 inhabitants, located about 50 km to the west of the station.

In order to monitor the NPF events, a TROPOS type custom-built Scanning Mobility Particle Sizer (SMPS), similar to IFT-SMPS in Wiedensohler et al. (2012), was used at Finokalia. Particle number size distributions were measured in the diameter range of 9–848 nm every five minutes. The system was a closed-loop, with a 5:1 ratio between the aerosol and sheath flow and it consisted of a Kr-85 aerosol neutralizer (TSI 3077), a Hauke medium Differential Mobility Analyzer (DMA) and a TSI-3772 Condensation Particle Counter (CPC). The sampling was made through a PM₁₀ sampling head and the sample humidity was regulated below the relative humidity of 40% with the use of Nafion® dryers in both the aerosol and sheath flow. The measured number size distributions were corrected for particle losses by diffusion on the various parts of the SMPS according to the methodology described in Wiedensohler et al. (2012). Three different types of calibration were performed for the SMPS, DMA voltage supply calibration, aerosol and sheath flows calibrations and size calibrations. These measurements

have been performed at Finokalia on a continuous basis since 2008. The instrument used at Finokalia was audited on-site with good results in the framework of EUSAAR (European Supersites for Atmospheric Aerosol Research) project (<http://www.wmo-gaw-wcc-aerosol-physics.org/audits.html>) and has successfully passed twice laboratory intercomparison workshops (2013 and 2016, reports available at <http://www.wmo-gaw-wcc-aerosol-physics.org/instrumental-workshops.html>) in the framework of ACTRIS project. The instrument has been operated following the recommendations described in Wiedensohler et al. (2012). Additional information for newly formed particles were obtained with the use of an Air Ion Spectrometer (AIS- AIREL Ltd., Institute of Environmental Physics, University of Tartu, Estonia, Mirme et al., 2007). AIS is a cluster ion air spectrometer used to simultaneously measure electrical mobility distribution of positive and negative air ions (mobilities in the range of 2.4 to $1.3 \cdot 10^{-3} \text{ cm}^2 \text{ V}^{-1} \text{ s}^{-1}$). The mobility distributions were then transformed to size distributions in the size range 0.8-42 nm. The number counting threshold was approximately 10 cm^{-3} and the uncertainties of the AIS measurements were ~10% for negative and positive ion concentrations and ~0.5 nm in size (Manninen et al., 2010). The diameter of the AIS inlet tube was 35 mm and the sample flow rate was 60 L m^{-1} . The time step of the measurements was five minutes.

These measurements have been used to identify NPF for the whole period and provide a historical perspective for the frequency and the characteristics of NPF phenomena in the eastern Mediterranean. Calculations for formation rates of new particles (J), growth rates (GR) in various size ranges and condensation sink (CS) were made according to Kulmala et al. (2012). Formation rates of particles with diameter D_p (in this study $D_p=9\text{nm}$) were calculated as:

$$J_{Dp} = \frac{\Delta N_{Dp}}{\Delta t} + CoagS_{Dp} \cdot N_{Dp} + \frac{GR}{\Delta D_p} \cdot N_{Dp} + S_{losses} \quad (1)$$

ΔN_{Dp} is the increase in nucleation mode particles' number concentration ($D_p < 25\text{nm}$), $CoagS_{Dp}$ is the coagulation of 9nm particles on larger particles, GR is the growth rate in the size range 9-25nm. S_{losses} takes into account additional losses and was neglected in this study. GR was calculated using the mode-fitting method (Dal Maso et al., 2005). The aerosol size distributions were fitted with lognormal distributions and the nucleation mode geometric mean diameter was plotted as a function of time. GR was calculated as the slope of the linear fit so that:

$$GR = \frac{dD_p}{dt} (2)$$

CS is the condensation sink caused by the pre-existing aerosol population and was calculated using the properties of sulfuric acid as condensing vapor.

All important meteorological parameters were monitored every five minutes using an automated meteorological station, including the temperature, wind velocity and direction, relative humidity, solar irradiance and precipitation. Ozone concentrations were measured with a TEI 49C instrument and nitrogen oxides with a TEI 42CTL, both commercially available, with a time step of five minutes.

2.2) NPF simulations with the MALTE-Box model

The simulations of NPF events in the eastern Mediterranean atmosphere were here performed using the MALTE-box model of the University of Helsinki. This 0-d model able to simulate aerosol dynamics and chemical processes has successfully reproduced observations of aerosol formation and growth in the boreal environment (Boy et al., 2006) as well as in highly polluted areas (Huang et al., 2016). For the present study, chemical reactions relevant to the production of condensing species from the Master Chemical Mechanism were incorporated in the MALTE-box chemical mechanism, as described in Boy et al. (2013). These include the full MCM degradation scheme of the following volatile organic compounds (described in more detail in Tzitzikalaki et al., 2017): C₁-C₄ alkanes, C₂-C₃ alkenes, acetylene, isoprene, α- and β-pinene, aromatics, methanol, dimethyl sulfide, formaldehyde, formic and acetic acids, acetaldehyde, glycoaldehyde, glyoxal, methylglyoxal, acetone, hydroxyacetone, butanone and marine amines. The Kinetic PreProcessor (KPP) was used to produce the Fortran code for the calculations of the concentrations of each individual compound (Damian et al., 2002), except for those species whose concentrations were manually input from large scale model simulations.

The major aerosol dynamical processes for clear sky atmosphere were simulated by the size-segregated aerosol model UHMA (University Helsinki Multicomponent Aerosol Model, Korhonen et al., 2004) impended in the MALTE-Box model. Measured aerosol number size distributions were used to initialize UHMA daily, which simulates NPF, coagulation, growth and dry deposition of particles. UHMA simulated new cluster formation using the activation nucleation parameterization, so that the nucleation rate has a linear relationship with sulfuric acid concentration, depending on the nucleation coefficient K_{act}.

1 Apart from sulfuric acid, about 20 extremely low-volatility organic compounds (ELVOCs) and
2 7 selected semi-volatile organic compounds (SVOCs) were treated as condensing vapors,
3 following the simplified chemical mechanism presented in Huang et al. (2016). All condensing
4 compounds were treated either as sulfuric acid or organic compounds and the condensation
5 of organic vapors was determined by the nano-Kohler theory (Kulmala et al., 2004b).

6 As input to the MALTE-Box model were used the observations at Finokalia station and when
7 such observations were not available, the results from numerical simulations with the global
8 3-dimensional chemistry transport model (CTM) TM4-ECPL (Daskalakis et al., 2015, 2016;
9 Myriokefalitakis et al., 2010, 2016) for Finokalia. Observational data include temperature,
10 relative humidity, total radiation (meteorological input), ozone (O₃) and nitrogen oxides (NO_x)
11 concentrations as well as aerosol number size distributions. The aerosol number size
12 distribution measured by the SMPS was used to calculate the condensation sink for H₂SO₄
13 vapors. Due to the lack of detailed measurements of VOC at Finokalia, as a first approximation,
14 biogenic and anthropogenic concentrations of all the above mentioned VOCs resolved every
15 3 hours were taken from the TM4-ECPL model.

16 The global TM4-ECPL model was run driven for this study by ECMWF (European Centre for
17 Medium – Range Weather Forecasts) Interim re-analysis project (ERA – Interim) meteorology
18 (Dee et al., 2011) of the year 2012 at an horizontal resolution of 3° in longitude x 2° in latitude
19 with 34 vertical layers up to 0.1 hPa. The model used year-specific meteorology and emissions
20 of trace gases and aerosols. For this study, that of the year 2012 was used, except for soil NO_x
21 and oceanic CO and VOCs emissions which were taken from POET inventory database for the
22 year 2000 (Granier et al., 2005). TM4-ECPL simulations for this work were performed with a
23 model time-step of 30 min, and the simulated VOC concentrations every 3-hours were used
24 as input to MALTE box model; while SO₂ surface levels at Finokalia were taken from Monitoring
25 Atmospheric Composition and Climate (MACC) data assimilation system (Inness et al., 2013).

26 For the calculations of the photo-dissociation rate coefficient by the MALTE-Box model, the
27 solar actinic flux (AF) is needed. Unfortunately, AF was not measured at Finokalia in 2012,
28 therefore AF levels were calculated by the Tropospheric Ultraviolet and visible Radiation
29 Model (TUV, Madronich, 1993) version v.5 for cloud free conditions. The ability of TUV to
30 calculate the AF at Finokalia was investigated by comparing observations of photo dissociation
31 rates of O₃ (JO¹D) and NO₂ (JNO₂) and model calculations. The measurements of these photo
32 dissociation rates were performed by filter radiometers (Meteorologie Consult, Germany).

1 The JO¹D was measured at wavelengths <325nm, while for JNO₂ wavelengths <420nm were
2 used.

3 A series of sensitivity tests of AF to different input parameters was also performed to optimize
4 the calculations. The model uses extra-terrestrial solar spectral irradiance (200-1000 nm by
5 0.01nm steps) and computes its propagation through the atmosphere taking into account
6 multiple scattering and the absorption and scattering due to gases and particles. TUV inputs
7 of interest were surface reflectivity (albedo), O₃ column, Aerosol Optical Depth at 500nm
8 (AOD), Single Scattering Albedo of aerosol (SSA), NO₂ column, air density. Total O₃ column
9 values were taken from Ozone Monitoring Instrument (OMI) on the Aura spacecraft of NASA
10 (Levelt et al., 2006). Aerosol columnar optical properties were obtained from the Aerosol
11 Robotic Network (AERONET). AOD data were measured at the FORTH_Crete station which is
12 located 35 km west of Finokalia (Fotiadi et al., 2006). Data level 1.5 was used (cloud-screened).
13 Total NO₂ column values were taken from GOME2 and OMI satellites. The calculations were
14 carried out at wavelength from 280 to 650nm with a resolution of 5nm. Simulations using
15 surface reflectivity of 0.075 and simulation using O₃ column taken from OMI had the best
16 correlation with measurements. However, the TUV model still significantly overestimated
17 JO¹D and JNO₂ data. Thus, a parameterisation took place following a simple empirical
18 approach, according to Mogensen et al. (2015) and the ratios between the measured and
19 modelled (from TUV) photolysis rate were calculated and used in the model.

20 3) Results and discussion

21 3.1) Particle size distribution and its connection with NPF

22 We analyzed all available measurements of number size distributions of atmospheric aerosol
23 particles measured at Finokalia in order to identify and analyze the NPF phenomenon in the
24 eastern Mediterranean. The data coverage for the period 2008-2018 was 82 %, providing one
25 of the longest time series of size distributions not only in this region but also in the southern
26 Europe and a unique data base for aerosol physical properties.

27 First, we calculated the total particle number concentration (median concentration was
28 2202 cm⁻³, standard deviation (SD) 528 cm⁻³) and corresponding number concentration in the
29 nucleation mode ($d_p < 25\text{nm}$, median 80 cm⁻³, SD 528 cm⁻³), Aitken mode ($25\text{nm} < d_p < 100\text{nm}$,
30 median 1028 cm⁻³, SD 894 cm⁻³) and accumulation mode ($d_p > 100\text{nm}$, median 898 cm⁻³, SD
31 605 cm⁻³). We found that Aitken mode accounted for 50% and accumulation mode 42% of the
32 total particle number concentration, while the nucleation mode accounted only for 8%. The

standard deviation of the nucleation particle number concentration was 528 cm^{-3} , indicating that the abundance of these smallest particles is of episodic nature. The highest monthly average concentrations of nucleation mode particles were observed during winter and early spring and the lowest ones during summer (Figure 1a). Calculating the median diurnal variability of the nucleation mode, we can see that there is a clear pattern for all seasons of the year (Figure 2a) with a sudden burst in the number concentration around noon that is most pronounced in winter and least in summer. Such an observation suggests that the nucleation particle number concentration is controlled by NPF episodes rather than other sources such as combustion processes. As can be seen in Figure 2b where a typical “banana shaped” pattern of an NPF event at Finokalia is presented, the sudden burst at noon is typical for a NPF event. In summer, nucleation mode particles have the highest concentrations during the night, yet another concentration relative maximum at noon can be attributed to NPF (Figure 2a). The shift in the average time of the daytime burst of nucleation mode particles can be attributed to the annual variation of the daylight length. Similar observations to ours have been reported in Cusack et al. (2013) for the western Mediterranean where the diurnal variation of nucleation mode particles presents a clear maximum at noon under both polluted and clean conditions.

It is worth noticing that during night-time the median nucleation mode particle number concentrations were similar in all the seasons. This suggests that there is some new particle production mechanism at night, especially in summer and autumn, that operates separately from daytime NPF. Frequently during the night-time, we observed a pronounced appearance of new nucleation mode particles over several hours as illustrated by Figure 3. While nocturnal NPF has been reported in the literature (see Salimi et al. (2017) and references therein), this phenomenon seems to be rare and it remains unclear what are the exact mechanisms leading to it. Given that we observed no or little growth during nighttime NPF, we may assume that the sources leading to the formation of new particles are local rather than regional and that the lack of photochemistry during night limits the abundance of condensable vapors driving particle growth. Observations of very localized NPF have been reported in Mace Head, Ireland, where intense NPF frequently takes place under low tide conditions when algae are exposed to the atmosphere (O’Dowd et al., 2002). Henceforth, we will exclude the nighttime NPF events from our further analysis. We refer the interested reader to Kalivitis et al. (2012) for a more detailed description of this phenomenon.

1 Overall, we observed atmospheric NPF to take place during both day and night at Finokalia,
2 but no sign of any other source of nucleation mode particles in measured air masses. We
3 therefore hypothesize that atmospheric NPF is the dominant source of nucleation mode
4 particles in this Mediterranean environment.

5 3.2) Characteristics of NPF in the eastern Mediterranean

6 We analyzed the dataset of aerosol size distributions following the approach of Dal Maso et
7 al. (2005) in order to mark the available days as 1) NPF event days when a clear new nucleation
8 mode and subsequent growth of newly-formed particles to larger diameters can be observed,
9 2) non-event days and 3) undefined days when either new particles appear into the Aitken
10 mode or nucleation mode particles do not show a clear growth. The available days were
11 manually inspected and classified.

12 We used the Statistica software package for Windows to carry out factor analyses, including
13 meteorological parameters, ozone concentrations (as an important oxidant in the
14 atmosphere) and PM₁₀ mass concentration (as an index of particulate pollutant levels), in
15 order to examine whether any of these factors were associated with the formation of new
16 particles, represented by the nucleation mode number concentration. Furthermore, we
17 divided our data to night and day time periods in order to separate daytime NPF from that
18 taking place during nighttime. The only parameter that had some effect on the nucleation
19 mode particle number concentration was the wind velocity: when strong winds were
20 prevailing at Finokalia, it was more unlikely to observe nucleation particles. On the other hand,
21 the lack of correlation to any other parameter may indicate that the NPF is not sensitive to
22 local meteorological conditions, preexisting particulate matter and ozone levels in this
23 environment. Air mass back trajectories calculated using the HYSPLIT model showed little
24 difference during NPF events from air masses typical for the prevailing situation at Finokalia:
25 air masses arriving at Finokalia from the northeast were the most frequent during NPF events
26 (30% against 24% of all days), followed by northern directions (20% against 21%) and
27 northwestern air masses that were more frequent than the average (19% against 17%).

28 Next, we focused on determining the main characteristics of daytime NPF at Finokalia. Overall,
29 837 NPF events were identified. This is the longest time series of the NPF phenomenon
30 recorded in the Mediterranean atmosphere, providing a representative climatology of NPF
31 events in this region. NPF took place 27% of the 3057 available measurement days whereas
32 no event occurred on 50% of those days. It is worth noting that 23% of the days were

1 characterized as undefined, which means that while no clear NPF event could be observed,
2 there was some evidence of secondary particle formation although not at the immediate
3 vicinity of the station (Table 1). We found that NPF is most frequent in April and May, probably
4 due to the biogenic activity and the onset of intense photochemistry, and least frequent in
5 August (Figure 4) probably due to high wind speeds occurring these month (not shown) and
6 additionally the high Condensational Sink (Figure 1b). Rain season in southeastern Europe in
7 early autumn leads to gradual CS decrease, and as a result a local maximum in NPF frequency
8 is observed in October. NPF at Finokalia takes place throughout the year.

9 As a next step, we classified the NPF events into Class I or Class II events depending on whether
10 the particle formation rate at 9 nm (J_9) and growth rates from 9 to 25 nm diameter (GR_{9-25})
11 could be calculated with a good confidence. Overall, Class I events corresponded to 8% of the
12 available measuring days and 28% of the event days, and they were observed throughout the
13 year, providing enough data for a statistical analysis of particle formation and growth rates
14 during NPF events (Figure 5).

15 The average value of J_9 during the Class I NPF events in Finokalia was $0.9 \text{ cm}^{-3} \text{ s}^{-1}$ (median 0.5
16 $\text{cm}^{-3} \text{ s}^{-1}$, SD $1.2 \text{ cm}^{-3} \text{ s}^{-1}$). This is well in the range of values reported for J_{10} in other locations
17 (Kulmala et al., 2004a), higher though than J_{16} reported by Berland et al. (2017) at the Finokalia
18 site in 2013 ($0.26 \text{ cm}^{-3} \text{ s}^{-1}$), but substantially lower than the values found by Kopanakis et al.
19 (2013) in western Crete ($13.1 \pm 9.9 \text{ cm}^{-3} \text{ s}^{-1}$). The monthly variation of J_9 (Figure 6a) shows that
20 the highest average formation rates were observed in December and January, probably as a
21 result of the low CS values observed in winter, although it is difficult to say which factors
22 determine the monthly variability of J_9 at Finokalia. Seasonal averages of J_9 , GR_{9-25} and CS are
23 summarized in Table 2. Moreover, we found that J_9 and N_{9-25} have a clear linear relation (Figure
24 7), which supports our earlier hypothesis that at Finokalia the main source of nucleation mode
25 particles is their secondary formation in the atmosphere.

26 We calculated the average growth rate of the newly formed particles to be 5.4 nm hr^{-1} (median
27 4.5 nm hr^{-1} , SD 3.9 nm hr^{-1}). We found that GR_{9-25} is highest in summer until September and
28 lowest in winter and early spring, probably in line with the seasonal cycle of photochemical
29 activity and biogenic emission patterns, producing condensable species that are driving the
30 growth process (Figure 6b). Additionally, transported pollution in summer at Finokalia may
31 contribute except of CS to GR as well, transported anthropogenic SO_2 may play a role in the
32 growth process as a precursor for sulfuric acid.

The survival probability of newly-formed particles is closely related to the ratio of CS to GR, at least for cluster sizes (Kerminen and Kulmala, 2002; Kulmala et al., 2017) and at Finokalia they present the same annual cycle. The survival probability for nucleation mode particles for Class I events was calculated based on the formula in Kulmala et al. (2017). It was found that on seasonal basis the median survival probability is higher in summer and winter, however varies between the seasons only within 5%. The concentrations of nucleation mode particles are lower during summer and the average duration of the NPF in summer seems to be shorter as shown in Figures 1 and 2a respectively. These observations may be explained by the higher CS and GR during summer. The CS (and hence CoagS) may directly affect the maximum concentrations observed. The slightly higher survival probability in summer explains perhaps that given the high CS, in order for new particles to survive the need to grow fast. On the other hand, one would expect NPF to be most frequent in winter when the highest concentrations of nucleation particles are observed and CS is the lowest, however this was not the case. A possible explanation for the high nucleation mode particle number concentrations in winter could be that the survival probability is higher than in spring or autumn.

3.3) NPF trends during the 2008-2018 period

During the period under study no statistically significant trends in NPF events were observed at Finokalia for the 120 available months. It should be noted though, that since 2010 a decreasing trend is observed, which is statistically significant with a p-value of 0.005. During the measurement period under study, no trend in J_9 was observed (Figure 8c). Although no statistically significant trend was observed for GR_{9-25} as well (Figure 8d), we observed a decreasing trend during the period 2008-2015 of about $0.3 \text{ nm hr}^{-1} \text{ yr}^{-1}$. This trend can be considered statistically significant (p-value of 0.03). In order to explain this trend, we need to emphasize the regional characteristics of the observations at Finokalia, as this site is greatly affected by long-range transported pollutants of marine, desert dust and polluted continental origin (Lelieveld et al., 2002). Non-sea salt sulfate ($nss\text{-SO}_4^{2-}$) can be considered as an indicator of regional pollution from anthropogenic activities (SO_2 emissions), and since the beginning of the economic crisis in Europe, especially in Greece, we observed a clear decline in its concentration since 2008 (Paraskevopoulou et al., 2015) which however has stopped after 2015. We can therefore assume also a regional decrease in SO_2 emissions, since the main source of SO_2 at Finokalia is attributed to transported pollution (Sciare et al., 2003). This could

1 result in a decrease in the availability of sulfuric acid, a major condensable species responsible
2 for the particle growth (Bzdek et al., 2012).

3 Hamed et al. (2010) studied the effect of the reduction in anthropogenic SO₂ emissions in
4 Germany between the years 1996-97 and 2003-06 as a result of the socio-economic changes
5 in East Germany after the reunification. They observed a notable decrease in the NPF event
6 frequency but an increase in the growth rate of nucleated particles. A decrease in the NPF
7 frequency due to the reduction of anthropogenic SO₂ emissions in eastern Lapland was also
8 reported by Kyrö et al. (2014), and this decrease was most pronounced for the Class I NPF
9 events. Nieminen et al. (2014) analyzed the longest data set reported in literature from
10 Finland and found that, despite major decreases in ambient SO₂ concentrations observed all
11 over Europe as a result of overall air quality improvements, there was a slight upward trend
12 in the particle formation and growth rates. This feature was attributed partly to increased
13 biogenic emissions over the same period.

14 In our case the reasons for the variations in the NPF frequency, J_9 and GR₉₋₂₅ remain unclear,
15 even though factors like meteorological conditions and organic vapor abundance have
16 probably played some role in this respect.

17 3.4) Atmospheric ion observations related to new particle formation

18 At the Finokalia station, atmospheric ion observations relevant to new particle formation were
19 performed during two separate periods, 2008-2009 during the EUCAARI project (Manninen et
20 al., 2010) and 2012-2014 during the FRONT (Formation and growth of atmospheric
21 nanoparticles) project. Here we will focus only on FRONT data, since the EUCAARI dataset is
22 discussed in detail in Manninen et al. (2010) and Pikridas et al., (2012). A typical nucleation
23 event is presented in Fig. 9 as recorded by both the AIS and SMPS. AIS observations may
24 provide information about the initial stages of new particle formation as particles can be
25 observed emerging in the intermediate ion diameter range 1.6-7.4 nm. Intermediate ions
26 appear only under certain circumstances, such as during precipitation, at high wind speeds,
27 and when NPF is taking place (Hörrak et al. 1998; Tamm et al., 2014; Leino et al., 2016; Chen
28 et al., 2017). In the following we will focus on NPF and use only the observations from the
29 negative polarity due to the better representation of NPF events in those data compared with
30 corresponding positive ions in our dataset (Kalivitis et al., 2012).

31 We classified all of the available AIS measurement days into event, non-event and undefined
32 days, once again according to methods introduced by Dal Maso et al. (2005), and subsequently

1 compared the findings from AIS data to those from the SMPS. In Figure 9 an NPF event is
2 presented observed with both the AIS and the SMPS at Finokalia. Surprisingly, the two data
3 sets for the same time period gave quite different results in terms of the NPF event frequency:
4 in the AIS data the NPF event frequency peaked earlier during the year than in the SMPS data
5 (Figure 10). This feature was evident in both periods of AIS measurements and is probably due
6 and has been also reported at a rural site in Hungary (Yli-Juuti et al., 2009), probably because
7 AIS detects only naturally charged particles while SMPS all particles. Additionally, it is possible
8 that AIS data are more representative of local NPF events with limited particle growth, and
9 such events may not be seen in the SMPS data. On the other hand, the SMPS measures neutral
10 particles but has a much higher detection limit (9nm), so its data may be more representative
11 of regional NPF that takes place over distances of hundreds of kilometers (Kalkavouras et al.,
12 2017).

13 We calculated the growth rates at three different size ranges for the FRONT project similarly
14 to Manninen et al. (2010) and Pikridas et al (2012) for the EUCAARI project data. The particle
15 growth rates in the size ranges 1.5-3 nm, 3-7nm and 7-20 nm were $1.6 \pm 1.8 \text{ nm hr}^{-1}$, 5.4 ± 4.9
16 nm hr^{-1} and $9.1 \pm 9.5 \text{ nm hr}^{-1}$, respectively. These values are lower than those in Pikridas et al.
17 (2012) but comparable to those observed during the EUCAARI project for the first two size
18 ranges, and higher than those observed during the EUCAARI project for the last size range
19 (Manninen et al., 2010). Overall, we observed much faster growth of newly-formed charged
20 particles in the eastern Mediterranean atmosphere after their first growth steps beyond 3 nm
21 in diameter, reflecting probably the strong Kelvin effect at small particle sizes preventing
22 condensation and hence growth, and the abundance of precursors leading to nucleation and
23 condensing species contributing to each growth stage.

24 3.5) Simulations of NPF using the zero-dimensional model MALTE-box

25 In order to evaluate our understanding of the observed NPF events in the eastern
26 Mediterranean we chose to simulate two distinct cases of one week duration each, during
27 which NPF events have been observed (event week) or not (no event week). The selection was
28 done from the summer of the year 2012, when JO^1D and JNO_2 photodissociation
29 measurements were also available at Finokalia. Two weeks in August 2012 were chosen,
30 28/08– 03/09 as event week and 09/08– 15/08 as non-event week. The “event week” was
31 described in detail by Kalivitis et al. (2015). Applying the MALTE-Box model the aerosol size
32 distribution and its evolution over the week has been simulated for these two cases.

During the “event week” the simulated formation of new particles successfully coincided with the observations. The NPF events simulated using the nucleation rates as parameterized for the boreal environment overestimated the observations while the simulated growth of newly-formed particles was greatly underestimated as shown in Tzitzikalaki et al. (2017). The most likely reason for this is the very low concentration of monoterpenes, calculated by TM4-ECPL global model for the Finokalia model grid box, on which the ELVOC and SVOC chemistry was built on. Indeed, the TM4-ECPL model results for Finokalia were too low compared to monoterpenes observations in 2014 (not shown). Therefore, we performed a number of sensitivity tests to improve the simulations by adjusting the nucleation coefficient and the monoterpene concentrations until we simulated efficiently the nucleation and growth rates observed during the second day of the “event week” when the most pronounced NPF event was observed. The best agreement between model results and observations was reached by decreasing the nucleation coefficient from 10^{-11} s^{-1} (the value commonly used for the boreal environment) to $5 \times 10^{-16} \text{ s}^{-1}$ and increasing by a factor of 10 the α - and β -pinene concentrations. With these modifications the model results improved and the aerosol number size distributions were better simulated, as well as total number and volume concentration of aerosol particles (Figures 11a and b respectively). This was the first time that we were able to simulate NPF in the eastern Mediterranean environment. The almost five orders of magnitude lower nucleation coefficient used here for the sub-tropical set-up could be related to the contribution of still unknown compounds in the cluster-formation process. Huang et al. (2016) applied different kinetic nucleation coefficients at Nanjing, China, with the lowest value for a “China-clean” day of $6.0 \times 10^{-13} \text{ s}^{-1}$. The higher monoterpene concentrations used are comparable to the findings at Finokalia but also to another location in eastern Mediterranean (Debevec et al., 2018).

Using the non-event week as our control case, we performed simulations of number size distributions at Finokalia station using the sub-tropical set-up and compared it to our measurements. For the “non-event week”, weak NPF were predicted by the model during the last two days that were not found in the measurements (Tzitzikalaki et al., 2017) but appear to be associated with the rapid drop of CS during day five of the simulations. Nevertheless, even if no NPF took place during the last two days, it was apparent in our measurements that some nucleation particles appeared ($\sim 200 \text{ cm}^{-3}$) and thus the general tendency was captured by the model. Both total number and volume concentrations were adequately simulated by the model (Figures 12 a, b). These results show the potential of MALTE-box model to simulate the NPF in the eastern Mediterranean and the importance of input data. Therefore, when

more appropriate input data for Malte-box will become available (concurrent detailed measurements of gases and aerosol distributions) at Finokalia, new simulations and VOC measurements will further provide insight in the nucleation mechanisms, the growth process and the factors controlling NPF in the eastern Mediterranean atmosphere.

4) Conclusions

NPF in the atmosphere is a recurrent phenomenon in eastern Mediterranean. In this study, we presented the longest time series of NPF records in the region. We analyzed 3057 days of aerosol number size distribution data from June 2008 until June 2018 and found that NPF took place 27% of the available days, more frequently in spring and less frequently in late summer. Production of nucleation mode particles was common during night-time as well. Nucleation mode particle number concentrations were low outside periods of active NPF and subsequent particle growth indicating absence of local sources. Classification of NPF events based on atmospheric ion measurements differed from the corresponding classification based on mobility spectrometer measurements: the maximum frequency of NPF events was observed earlier in spring from AIS data than from SMPS data, possibly indicating a different representation of local and regional NPF events between these two data sets since SMPS measures new particles after they have grown to diameters larger than 9nm and hence records only regional events lasting for several hours.

We used the MALTE-box model to simulate NPF observations in the eastern Mediterranean region. Using a “sub-tropical” environment parametrization, we were able to simulate with good agreement the selected time period. The parametrization used was significantly different than the one used for the boreal environment: nucleation rates were much lower, yet monoterpenes seemed to play a key role in the mechanisms governing NPF phenomena.

From the results presented in this work it is evident that the Finokalia site is a unique location in the eastern Mediterranean for studying the processes leading to NPF in the marine environment. As a next step, a more detailed look to the precursors driving these processes is necessary, with special emphasis on VOCs, and the expansion of the available measurements at the site in order to eliminate the uncertainties introduced in our simulations from the use of model outputs instead of observations.

1 5) Acknowledgements

2 The research project was implemented within the framework of the Action «Supporting
3 Postdoctoral Researchers» of the Operational Program "Education and Lifelong Learning"
4 (Action's Beneficiary: General Secretariat for Research and Technology), and was co-financed
5 by the European Social Fund (ESF) and the Greek State. This research is supported by the
6 Academy of Finland Center of Excellence program (project number 1118615). We
7 acknowledge funding from the EU FP7-ENV-2013 program "impact of Biogenic vs.
8 Anthropogenic emissions on Clouds and Climate: towards a Holistic UnderStanding"
9 (BACCHUS), project no. 603445 and the Horizon 2020 research and innovation programme
10 ACTRIS-2 Integrating Activities (grant agreement No. 654109). This study contributes to
11 ChArMEx work package 1 on aerosol sources.

12

1 6) References

- 2 Berland, K., Rose, C., Pey, J., Culot, A., Freney, E., Kalivitis, N., Kouvarakis, G., Cerro, J. C.,
 3 Mallet, M., Sartelet, K., Beckmann, M., Bourriane, T., Roberts, G., Marchand, N.,
 4 Mihalopoulos, N., and Sellegri, K.: Spatial extent of new particle formation events over the
 5 Mediterranean Basin from multiple ground-based and airborne measurements, *Atmos. Chem.*
 6 *Phys.*, 17, 9567-9583, <https://doi.org/10.5194/acp-17-9567-2017>, 2017.
- 7 Boy, M., Hellmuth, O., Korhonen, H., Nillson, D., ReVelle, D., Turnipseed, A., Arnold, F. and
 8 Kulmala, M.: MALTE – Model to predict new aerosol formation in the lower troposphere,
 9 *Atmos. Chem. Phys.*, 6, 4499–4517, doi:10.5194/acp-6-4499-2006, 2006.
- 10 Boy, M., Mogensen, D., Smolander, S., Zhou, L., Nieminen, T., Paasonen, P., Plass-Dülmer, C.,
 11 Sipilä, M., Petäjä, T., Mauldin, L., Berresheim, H., and Kulmala, M.: Oxidation of SO₂ by
 12 stabilized Criegee intermediate (sCI) radicals as a crucial source for atmospheric sulfuric acid
 13 concentrations, *Atmos. Chem. Phys.*, 13, 3865-3879, [https://doi.org/10.5194/acp-13-3865-](https://doi.org/10.5194/acp-13-3865-2013)
 14 2013, 2013.
- 15 Bzdek, B. R., Zordan, C. A., Pennington, M. R., Luther, G. W., and Johnston, M. V.: Quantitative
 16 Assessment of the Sulfuric Acid Contribution to New Particle Growth. *Environmental Science*
 17 *& Technology*, 46, 4365–4373. <http://doi.org/10.1021/es204556c>, 2012.
- 18 Chen, X., Virkkula, A., Kerminen, V.-M., Manninen, H. E., Busetto, M., Lanconelli, C., Lupi, A.,
 19 Vitale, V., Del Guasta, M., Grigioni, P., Väänänen, R., Duplissy, E.-M., Petäjä, T., and Kulmala,
 20 M.: Features of air ions measured by an air ion spectrometer (AIS) at Dome C, *Atmos. Chem.*
 21 *Phys.*, 17, 13783-13800, 2017.
- 22 Cusack, M., Pérez, N., Pey, J., Wiedensohler, A., Alastuey, A., and Querol, X.: Variability of sub-
 23 micrometer particle number size distributions and concentrations in the Western
 24 Mediterranean regional background. *Tellus B*, 65.
 25 doi:<http://dx.doi.org/10.3402/tellusb.v65i0.19243>, 2013.
- 26 Dall'Osto, M., Beddows, D. C. S., Asmi, A., Poulain, L., Hao, L., Freney, E., Allan, J D.,
 27 Canagaratna, M., Crippa, M., Bianchi, F., de Leeuw, G., Eriksson, A., Swietlicki, E., Hansson, H
 28 C., Henzing, J S., Granier, C., Zemankova, K., Laj, P., Onasch, T., Prevot, A., Putaud, J P., Sellegri,
 29 K., Vidal, M., Virtanen, A., Simo, R, Worsnop, D., O'Dowd, C., Kulmala, M. and Harrison, R.

1 M.:Novel insights on new particle formation derived from a pan-european observing system.
2 Scientific Reports, 8(1), 1482. <http://doi.org/10.1038/s41598-017-17343-9>, 2018.

3 Dal Maso, M., Kulmala, M., Riipinen, I., Wagner, R., Hussein, T., Aalto, P. P., and Lehtinen, K.
4 E. J.: Formation and growth of fresh atmospheric aerosols: eight years of aerosol size
5 distribution data from SMEAR II, Hyytiälä, Finland, Boreal Environ. Res., 10, 323–336, 2005.

6 Damian, V., Sandu, A., Damian, M., Potra, F., and Carmichael, G. R.: The kinetic preprocessor
7 KPP-a software environment for solving chemical kinetics, Computers & Chemical
8 Engineering, 26, 1567–1579, [http://doi.org/10.1016/S0098-1354\(02\)00128-X](http://doi.org/10.1016/S0098-1354(02)00128-X), 2002.

9 Daskalakis, N., Myriokefalitakis, S., and Kanakidou, M.: Sensitivity of tropospheric loads and
10 lifetimes of short lived pollutants to fire emissions, Atmos. Chem. Phys., 15, 3543-3563,
11 <https://doi.org/10.5194/acp-15-3543-2015>, 2015.

12 Daskalakis, N., Tsigaridis, K., Myriokefalitakis, S., Fanourgakis, G. S., and Kanakidou, M.: Large
13 gain in air quality compared to an alternative anthropogenic emissions scenario, Atmos.
14 Chem. Phys., 16, 9771-9784, doi:10.5194/acp-16-9771-2016, 2016.

15 Debevec, C., Sauvage, S., Gros, V., Sellegri, K., Sciare, J., Pikridas, M., Stavroulas, I., Leonardis,
16 T., Gaudion, V., Depelchin, L., Fronval, I., Sarda-Esteve, R., Baisnée, D., Bonsang, B., Savvides,
17 C., Vrekoussis, M., and Locoge, N.: Driving parameters of biogenic volatile organic compounds
18 and consequences on new particle formation observed at an eastern Mediterranean
19 background site, Atmos. Chem. Phys., 18, 14297-14325, [https://doi.org/10.5194/acp-18-](https://doi.org/10.5194/acp-18-14297-2018)
20 14297-2018, 2018.

21 Dee, D. P., Uppala, S. M., Simmons, A. J., Berrisford, P., Poli, P., Kobayashi, S., and Vitart, F.:
22 The ERA-Interim reanalysis: configuration and performance of the data assimilation system,
23 Quarterly Journal of the Royal Meteorological Society, 137, 553–597.
24 <http://doi.org/10.1002/qj.828>, 2011.

25 Fotiadi, A., Hatzianastassiou, N., Drakakis, E., Matsoukas, C., Pavlakis, K. G., Hatzidimitriou, D.,
26 Gerasopoulos, E., Mihalopoulos, N., and Vardavas, I.: Aerosol physical and optical properties
27 in the eastern Mediterranean Basin, Crete, from Aerosol Robotic Network data, Atmos. Chem.
28 Phys., 6, 5399-5413, <https://doi.org/10.5194/acp-6-5399-2006>, 2006.

29 Gordon, H., Kirkby, J., Baltensperger, U., Bianchi, F., Breitenlecher, M., Curtius, J., Dias, A.,
30 Dommen, J., Donahue, N. M., Dunne, E. M., Duplissy, J., Ehrhart, S., Flagan, R. C., Frege, C.,

1 Fuchs, C., Hansel, A., Hoyle, C. R., Kulmala, M., Kürten, A., Lehtipalo, K., Makhmutov, V.,
2 Molteni, U., Rissanen, M. P., Stozkhov, Y., Tröstl, J., Tsagkogeorgas, G., Wagner, R., Williamson,
3 C., Wimmer, D., Winkler, P. M., Yan, C., and Carslaw, K. S.: Causes and importance of new
4 particle formation in the present-day and preindustrial atmospheres, *J. Geophys. Res. Atmos.*,
5 122, 8739-8760, 2017.

6 Granier, C., Guenther, A., Lamarque, J., Mieville, A., Müller, J., Olivier, J., Orlando, J., Peters,
7 J., Petron, G., Tyndall, G., and Wallens, S.: POET, a database of surface emissions of ozone
8 precursors, available at: [http://www.aero.jussieu.fr/projet/](http://www.aero.jussieu.fr/projet/ACCENT/POET.php) ACCENT/POET.php, 2005.

9 Hamed, A., Birmili, W., Joutsensaari, J., Mikkonen, S., Asmi, A., Wehner, B., Spindler, G.,
10 Jaatinen, A., Wiedensohler, A., Korhonen, H., Lehtinen, K. E. J., and Laaksonen, A.: Changes in
11 the production rate of secondary aerosol particles in Central Europe in view of decreasing SO₂
12 emissions between 1996 and 2006, *Atmos. Chem. Phys.*, 10, 1071-1091,
13 <https://doi.org/10.5194/acp-10-1071-2010>, 2010.

14 Hörrak U., Salm J., and Tammet H.: Bursts of intermediate ions in atmospheric air, *J. Geophys.*
15 *Res.*, 103, 13909–13915, doi: 10.1029/97JD01570, 1998.

16 Huang, X., Zhou, L., Ding, A., Qi, X., Nie, W., Wang, M., Chi, X., Petäjä, T., Kerminen, V.-M.,
17 Roldin, P., Rusanen, A., Kulmala, M., and Boy, M.: Comprehensive modelling study on
18 observed new particle formation at the SORPES station in Nanjing, China, *Atmos. Chem. Phys.*,
19 16, 2477-2492, <https://doi.org/10.5194/acp-16-2477-2016>, 2016.

20 Inness, A., Baier, F., Benedetti, A., Bouarar, I., Chabrillat, S., Clark, H., Clerbaux, C., Coheur, P.,
21 Engelen, R. J., Errera, Q., Flemming, J., George, M., Granier, C., Hadji-Lazarou, J., Huijnen, V.,
22 Hurtmans, D., Jones, L., Kaiser, J. W., Kapsomenakis, J., Lefever, K., Leitão, J., Razinger, M.,
23 Richter, A., Schultz, M. G., Simmons, A. J., Suttie, M., Stein, O., Thépaut, J.-N., Thouret, V.,
24 Vrekoussis, M., Zerefos, C., and the MACC team: The MACC reanalysis: an 8 yr data set of
25 atmospheric composition, *Atmos. Chem. Phys.*, 13, 4073-4109, [https://doi.org/10.5194/acp-](https://doi.org/10.5194/acp-13-4073-2013)
26 13-4073-2013, 2013.

27 Kalivitis, N., Birmili, W., Stock, M., Wehner, B., Massling, A., Wiedensohler, A., Gerasopoulos,
28 E., and Mihalopoulos, N.: Particle size distributions in the eastern Mediterranean troposphere,
29 *Atmos. Chem. Phys.*, 8, 6729-6738, doi:10.5194/acp-8-6729-2008, 2008.

1 Kalivitis N., Stavroulas I., Bougiatioti A., Kouvarakis G., Gagné S., Manninen H.E., Kulmala M.,
2 and Mihalopoulos N.: Night-time enhanced atmospheric ion concentrations in the marine
3 boundary layer, *Atmos. Chem. Phys.*, 12, 3627-3638, doi:10.5194/acp-12-3627-2012, 2012.

4 Kalivitis, N., Kerminen, V.-M., Kouvarakis, G., Stavroulas, I., Bougiatioti, A., Nenes, A.,
5 Manninen, H. E., Petäjä, T., Kulmala, M., and Mihalopoulos, N.: Atmospheric new particle
6 formation as a source of CCN in the eastern Mediterranean marine boundary layer, *Atmos.*
7 *Chem. Phys.*, 15, 9203-9215, doi:10.5194/acp-15-9203-2015, 2015.

8 Kalkavouras, P., Bossioli, E., Bezantakos, S., Bougiatioti, A., Kalivitis, N., Stavroulas, I.,
9 Kouvarakis, G., Protonotariou, A. P., Dandou, A., Biskos, G., Mihalopoulos, N., Nenes, A., and
10 Tombrou, M.: New particle formation in the southern Aegean Sea during the Etesians:
11 importance for CCN production and cloud droplet number, *Atmos. Chem. Phys.*, 17, 175-192,
12 <https://doi.org/10.5194/acp-17-175-2017>, 2017.

13 Kerminen, V.-M. and Kulmala, M.: Analytical formulae connecting the “real” and the
14 “apparent” nucleation rate and the nuclei number concentration for atmospheric nucleation
15 events, *J. Aerosol Sci.*, 33, 609-622, 2002.

16 Kerminen, V.-M., Paramonov, M., Anttila, T., Riipinen, I., Fountoukis, C., Korhonen, H., Asmi,
17 E., Laakso, L., Lihavainen, H., Swietlicki, E., Svenningsson, B., Asmi, A., Pandis, S. N., Kulmala,
18 M., and Petäjä, T.: Cloud condensation nuclei production associated with atmospheric
19 nucleation: a synthesis based on existing literature and new results, *Atmos. Chem. Phys.*, 12,
20 12037– 12059, doi:10.5194/acp-12-12037-2012, 2012.

21 Kopanakis, I., Chatoutsidou, S. E., Torseth, K., Glytsos, T., and Lazaridis, M.: Particle number
22 size distribution in the eastern Mediterranean: Formation and growth rates of ultrafine
23 airborne atmospheric particles, *Atmospheric Environment*, 77, 790–802.
24 <http://doi.org/10.1016/j.atmosenv.2013.05.066>, 2013.

25 Korhonen, H., Lehtinen, K. E. J., and Kulmala, M.: Multicomponent aerosol dynamics model
26 UHMA: model development and validation, *Atmos. Chem. Phys.*, 4, 757-771,
27 <https://doi.org/10.5194/acp-4-757-2004>, 2004.

28 Kulmala, M., Vehkamäki, H., Petäjä, T., Dal Maso, M., Lauri, A., Kerminen, V.-M., Birmili, W.,
29 and McMurry, P. H.: Formation and growth rates of ultrafine atmospheric particles: A review
30 of observations, *J. Aerosol Sci.*, 35, 143–176, 2004a.

1 Kulmala, M, Kerminen, V.-M., Anttila, T., Laaksonen, A. and O'Dowd, C. D: Organic aerosol
2 formation via sulphate cluster activation, J. Geophys. Res., 109, 4205,
3 doi:10.1029/2003JD003961, 2004b.

4 Kulmala, M., Petäjä, T., Nieminen, T., Sipilä, M., Manninen, H. E., Lehtipalo, K., Kerminen, V.-
5 M.: Measurement of the nucleation of atmospheric aerosol particles, Nature Protocols, 7,
6 1651, <http://dx.doi.org/10.1038/nprot.2012.091>, 2012.

7 Kulmala, M., Petäjä, T., Ehn, M., Thornton, J., Sipilä, M., Worsnop, D. R., and Kerminen, V.-M.:
8 Chemistry of atmospheric nucleation: On the recent advances on precursor characterization
9 and atmospheric cluster composition in connection with atmospheric new particle formation,
10 Annu. Rev. Phys. Chem., 65, 21-37, 2014.

11 Kulmala, M., Kerminen, V.-M., Petäjä, T., Ding, A. J., and Wang L.: Atmospheric gas-to-particle
12 conversion: why NPF events are observed in megacities?, Faraday Discuss., 200, 271-288,
13 doi:10.1039/c6fd00257a, 2017.

14 Kyrö, E.-M., Väänänen, R., Kerminen, V.-M., Virkkula, A., Petäjä, T., Asmi, A., Dal Maso, M.,
15 Nieminen, T., Juhola, S., Shcherbinin, A., Riipinen, I., Lehtipalo, K., Keronen, P., Aalto, P. P.,
16 Hari, P., and Kulmala, M.: Trends in new particle formation in eastern Lapland, Finland: effect
17 of decreasing sulfur emissions from Kola Peninsula, Atmos. Chem. Phys., 14, 4383-4396,
18 <https://doi.org/10.5194/acp-14-4383-2014>, 2014.

19 Lazaridis, M., K. Eleftheriadis, J. Smolik, I. Colbeck, G. Kallos, Y. Drossinos, V. Zdimal, Z. Vecera,
20 N. Mihalopoulos, P. Mikuska, C. Bryant, C. Housiadas, A. Spyridaki, M. Astitha and V. Havranek:
21 Dynamics of fine particles and photo-oxidants in the eastern Mediterranean (SUB-AERO),
22 Atmospheric Environment, 40, P 6214-6228,
23 <http://dx.doi.org/10.1016/j.atmosenv.2005.06.050>, 2006.

24 Lehtipalo, K., Rondo, L., Kontkanen, J., Schobesberger, S., Jokinen, T., Sarnela, N., Kürten, A.,
25 Ehrhart, S., Franchin, A., Nieminen, T., Riccobono, F., Sipilä, M., Yli-Juuti, T., Duplissy, J.,
26 Adamov, A., Ahlm, L., Almeida, J., Amorim, A., Bianchi, F., Breitenlechner, M., Dommen, J.,
27 Downard, A. J., Dunne, E. M., Flagan, R. C., Guida, R., Hakala, J., Hansel, A., Jud, W.,
28 Kangasluoma, J., Kerminen, V.-M., Keskinen, H., Kim, J., Kirkby, J., Kupc, A., Kupiainen-Määttä,
29 O., Laaksonen, A., Lawler, M. J., Leiminger, M., Mathot, S., Olenius, T., Ortega, I. K., Onnela,
30 A., Petäjä, T., Praplan, A., Rissanen, M. P., Ruuskanen, T., Santos, F. D., Schallhart, S.,
31 Schnitzhofer, R., Simon, M., Smith, J. N., Tröstl, J., Tsagkogeorgas, G., Tomé, A., Vaattovaara,

1 P., Vehkamäki, H., Vrtala, A. E., Wagner, P. E., Williamson, C., Wimmer, D., Winkler, P. M.,
2 Virtanen, A., Donahue, N. M., Carslaw, K. S., Baltensperger, U., Riipinen, I., Curtius, J.,
3 Worsnop, D. R., and Kulmala, M.: The effect of acid-base clustering and ions on the growth of
4 atmospheric nano-particles, *Nat. Commun.*, 7, 11594, doi:10.1038/ncomms11594, 2016.

5 Leino, K., Nieminen, T., Manninen, H.E., Petäjä, T., Kerminen, V.-M., and Kulmala, M.:
6 Intermediate ions as a strong indicator for new particle formation bursts in a boreal forest.
7 *Boreal Env. Res.* 21: 274–286, 2016.

8 Lelieveld, J., Berresheim, H., Borrmann, S., Crutzen, P., Dentener, F., Fischer, H., Feichter, J.,
9 Flatau, P., Heland, J., Holzinger, R., Korrmann, R., Lawrence, M., Levin, Z., Markowicz, K.,
10 Mihalopoulos, N., Minikin, A., Ramanathan, V., de Reus, M., Roelofs, G., Scheeren, H., Sciare,
11 J., Schlager, H., Schultz, M., Siegmund, P., Steil, B., Stephanou, E., Stier, P., Traub, M., Warneke,
12 C., Williams, J., and Ziereis, H.: Global air pollution crossroads over the Mediterranean,
13 *Science*, 298, 794–799, doi: 10.1126/science.1075457, 2002.

14 Levelt, P. F., van den Oord, G. H. J., Dobber, M. R., Malkki, A., Visser, H., de Vries, J., Stammes,
15 P., Lundell, J. O. V., and Saari, H.: The Ozone Monitoring Instrument, *IEEE T. Geosci. Remote*,
16 44, 1093–1101, doi: 10.1109/TGRS.2006.872333, 2006.

17 Madronich, S.: The atmosphere and UV-B radiation at ground level. *Environmental UV*
18 *Photobiology*, Plenum Press, 1–39, 1993.

19 Manninen, H.E., Nieminen, T., Asmi, E., Gagné, S., Häkkinen, S., Lehtipalo, K., Aalto, P., Kivekäs
20 ,N., Vana, M., Mirme, A., Mirme, S., Hörrak, U., Plass-Dülmer, C., Stange, G., Kiss, G., Hoffer,
21 A., Moerman, M., Henzing, B., Brinkenberg, M., Kouvarakis, G.N., Bougiatioti, K., O’Dowd, C.,
22 Ceburnis, D., Arneth, A., Svenningsson, B., Swietlicki, E., Tarozzi, L., Decesari, S., Sonntag, A.,
23 Birmili, W., Wiedensohler, A., Boulon, J., Sellegri, K., Laj, P., Baltensperger, U., Laaksonen, A.,
24 Joutsensaari, J., Petäjä, T., Kerminen, V.-M., and Kulmala M.: EUCAARI ion spectrometer
25 measurements at 12 European sites – analysis of new particle formation events, *Atmos. Chem.*
26 *Phys.*, 10, 7907-7927, 2010.

27 Mihalopoulos, N., Stephanou, E., Kanakidou, M., Pilitsidis, S., and Bousquet, P.: Tropospheric
28 aerosol ionic composition in the eastern Mediterranean region, *Tellus Series B - Chemical and*
29 *Physical Meteorology*, 49, 314– 326, 1997.

1 Mirme, A., Tamm, E., Mordas, G., Vana, M., Uin, J., Mirme, S., Bernotas, T., Laakso, L., Hirsikko,
2 A. and M. Kulmala: A wide-range multi-channel Air Ion Spectrometer, *Boreal Environ. Res.*, 12,
3 247–264, 2007.

4 Mogensen, D., Gierens, R., Crowley, J. N., Keronen, P., Smolander, S., Sogachev, A., Nölscher,
5 A. C., Zhou, L., Kulmala, M., Tang, M. J., Williams, J., and Boy, M.: Simulations of atmospheric
6 OH, O₃ and NO₃ reactivities within and above the boreal forest, *Atmos. Chem. Phys.*, 15, 3909-
7 3932, <https://doi.org/10.5194/acp-15-3909-2015>, 2015.

8 Myriokefalitakis, S., Vignati, E., Tsigaridis, K., Papadimas, C., Sciare, J., Mihalopoulos, N.,
9 Facchini, M. C., Rinaldi, M., Dentener, F. J., Ceburnis, D., Hatzianastasiou, N., O'Dowd, C.D.,
10 van Weele, M., and Kanakidou, M.: Global modelling of the oceanic source of organic aerosols,
11 *Advances in Meteorology*, doi:10.1155/2010/939171, 2010.

12 Myriokefalitakis S., Daskalakis, N., Fanourgakis, G. S., Voulgarakis, A., Krol, M. C., Aan de Brugh,
13 J. M. J., and Kanakidou, M.: Pollution over the Mediterranean Basin: The Importance of Long-
14 Range Transport on ozone and carbon monoxide, *Science of The Total Environment*, 563–564,
15 40, 2016.

16 Nieminen, T., Asmi, A., Dal Maso, M., Aalto, P. P., Keronen, P., Petäjä, T., Kulmala, M., and
17 Kerminen, V.-M.: Trends in atmospheric new-particle formation: 16 years of observations in a
18 boreal-forest environment, *Boreal Env. Res.*, 19, 191-214, 2014

19 O'Dowd, C. D., Hämeri, K., Mäkelä, J. M., Pirjola, L., Kulmala, M., Jennings, S. G., Berresheim,
20 H., Hansson, H.-C., de Leeuw, G., Kunz, G. J., Allen, A. G., Hewitt, C. N., Jackson, A., Viisanen,
21 Y., and Hoffmann, T.: A dedicated study of New Particle Formation and Fate in the Coastal
22 Environment (PARFORCE): Overview of objectives and achievements, *J. Geophys. Res.*, 107,
23 8108, doi:10.1029/2001jd000555, 2002.

24 Paraskevopoulou, D., Liakakou, E., Gerasopoulos, E., and Mihalopoulos, N.: Sources of
25 atmospheric aerosol from long-term measurements (5 years) of chemical composition in
26 Athens, Greece. *Science of The Total Environment*, 527–528, 165–178.
27 <http://doi.org/10.1016/J.SCITOTENV.2015.04.022>, 2015.

28 Petäjä, T., Kerminen, V.-M., Dal Maso, M., Junninen, H., Koponen, I.K., Hussein, T., Aalto, P.P.,
29 Andronopoulos, S., Robin, D., Hämeri, K., Bartzis, J.G. and Kulmala, M.: Sub-micron
30 atmospheric aerosols in the surroundings of Marseille and Athens: physical characterization

1 and new particle formation, *Atmos. Chem. Phys.*, 7, pp. 2705-2720, doi:10.5194/acp-7-2705-
2 2007, 2007.

3 Pikridas, M., Riipinen, I., Hildebrandt, L., Kostenidou, E., Manninen, H., Mihalopoulos, N.,
4 Kalivitis, N., Burkhardt, J., Stohl, A., Kulmala, M. and Pandis, S. N.: NPF at a remote site in the
5 eastern Mediterranean, *J. Geophys. Res.*, 117, D12205, doi:10.1029/2012JD017570, 2012.

6 Sciare, J., Bardouki, H., Moulin, C., and Mihalopoulos, N.: Aerosol sources and their
7 contribution to the chemical composition of aerosols in the eastern Mediterranean Sea during
8 summertime, *Atmos. Chem. Phys.*, 3, 291-302, <https://doi.org/10.5194/acp-3-291-2003>,
9 2003.

10 Salimi, F., Rahman, M. M., Clifford, S., Ristovski, Z., and Morawska, L.: Nocturnal new particle
11 formation events in urban environments. *Atmos. Chem. Phys.*, 17, 521–530.
12 <http://doi.org/10.5194/acp-17-521-2017>, 2017.

13 Siakavaras, D., Samara, C., Petrakakis, M., and Biskos, G.: Nucleation events at a coastal city
14 during the warm period: Kerbside versus urban background measurements. *Atmospheric*
15 *Environment*, 140, 60–68. <http://doi.org/10.1016/j.atmosenv.2016.05.054>, 2016.

16 Spracklen, D. V., Carslaw, K. S., Kulmala, M., Kerminen, V.-M., Mann, G. W., and Sihto, S.-L.:
17 The contribution of boundary layer nucleation events to total particle concentrations on
18 regional and global scales, *Atmos. Chem. Phys.*, 6, 5631-5648, doi:10.5194/acp-6-5631-2006,
19 2006.

20 Tammet, H., Komsaare, K., and Hörrak, U.: Intermediate ions in the atmosphere, *Atmospheric*
21 *Research*, 135–136, 263–273, <http://doi.org/https://doi.org/10.1016/j.atmosres.2012.09.009>,
22 2014.

23 Tröstl, J., Chuang, W. K., Gordon, H., Heinritzi, M., Yan, C., Molteni, U., Ahlm, L., Frege, C.,
24 Bianchi, F., Wagner, R. and Simon, M., Lehtipalo, K., Williamson, C., Craven, J. S., Duplissy, J.,
25 Adamov, A., Almeida, J., Bernhammer, A.-K., Breitenlechner, M., Brilke, S., Dias, A., Ehrhart,
26 S., Flagan, R. C., Franchin, A., Fuchs, C., Guida, R., Gysel, M., Hansel, A., Hoyle, C. R., Jokinen,
27 T., Junninen, H., Kangasluoma, J., Keskinen, H., Kim, J., Krapf, M., Kürten, A., Laaksonen, A.,
28 Lawler, M., Leiminger, M., Mathot, S., Möhler, O., Nieminen, T., Onnela, A., Petäjä, T., Piel, F.
29 M., Miettinen, P., Rissanen, M. P., Rondo, L., Sarnela, N., Schobesberger, S., Sengupta, K.,
30 Sipilä, M., Smith, J. N., Steiner, G., Tomè, A., Virtanen, A., Wagner, A. C., Weingartner, E.,

1 Wimmer, D., Winkler, P. M., Ye, P., Carslaw, K. S., Curtius, J., Dommen, J., Kirkby, J., Kulmala,
2 M., Riipinen, I., Worsnop, D. R., Donahue, N. M., and Baltensperger, U.: The role of low-
3 volatility organic compounds in initial particle growth in the atmosphere, *Nature*, 533, 527–
4 531, 2016.

5 Tzitzikalaki, E., Kalivitis, N., Kouvarakis, G., Daskalakis, N., Kerminen, V.-M., Mihalopoulos, N.,
6 Boy, M., and Kanakidou, M.: Simulations of New Particle Formation and Growth Processes at
7 eastern Mediterranean, with the MALTE-Box Model, in: *Perspectives on Atmospheric*
8 *Sciences*. T. Karacostas, A. Bais, & P. T. Nastos (Eds.), (pp. 933–939). Cham: Springer
9 International Publishing, 2017.

10 Wang, Z., Wu, Z., Yue, D., Shang, D., Guo, S., Sun, J., Ding, A., Wang, L., Jiang, J., Guo, H., Gao,
11 J., Cheung, H. C., Morawska, L., Keywood, M., and Hu, M.: New particle formation in China:
12 Current knowledge and further directions, *Sci. Total Environ.*, 577, 258-266,
13 <http://dx.doi.org/10.1016/j.scitotenv.2016.10.177>, 2017.

14 Wiedensohler, A., Birmili, W., Nowak, A., Sonntag, A., Weinhold, K., Merkel, M., Wehner, B.,
15 Tuch, T., Pfeifer, S., Fiebig, M., Fjåraa, A. M., Asmi, E., Sellegri, K., Depuy, R., Venzac, H., Villani,
16 P., Laj, P., Aalto, P., Ogren, J. A., Swietlicki, E., Williams, P., Roldin, P., Quincey, P., Hüglin, C.,
17 Fierz-Schmidhauser, R., Gysel, M., Weingartner, E., Riccobono, F., Santos, S., Gröning, C.,
18 Faloon, K., Beddows, D., Harrison, R., Monahan, C., Jennings, S. G., O'Dowd, C. D., Marinoni,
19 A., Horn, H.-G., Keck, L., Jiang, J., Scheckman, J., McMurry, P. H., Deng, Z., Zhao, C. S.,
20 Moerman, M., Henzing, B., de Leeuw, G., Löschau, G., and Bastian, S.: Mobility particle size
21 spectrometers: harmonization of technical standards and data structure to facilitate high
22 quality long-term observations of atmospheric particle number size distributions, *Atmos.*
23 *Meas. Tech.*, 5, 657-685, doi:10.5194/amt-5-657-2012, 2012.

24 Yli-Juuti, T., Riipinen, N., Aalto, P.P., Nieminen, T., Maenhaut, W., Janssens, I.A., Claeys, M.,
25 Salma, I., Ocskay, R., Hoffer, A., Lmre, K. and Kulmala, M.: Characteristics of new particle
26 formation events and cluster ions at K-puszt, Hungary, *Boreal Environment Research*, vol. 14,
27 no. 4, pp. 683-698, 2009

28

1 7) Tables

Day classification	Number of events	%
Total events	837	27.4
Class I	232	7.6
Class II	605	19.8
Undefined	687	22.5
Non-event	1533	50.1
Total days	3057	100.00

2

3 Table 1) Total available measurement days and percentage of NPF events observed at
4 Finokalia during the period June 2008-June 2018

	J_9 ($\text{cm}^{-3} \text{s}^{-1}$)			GR_{9-25} (nm hr^{-1})			$\text{CS} \times 10^{-3}$ (s^{-1})		
	Mean	Median	SD	Mean	Median	SD	Mean	Median	SD
Winter	0.9	0.6	1.4	3.3	2.6	2.4	4.3	3.5	2.9
Spring	1.0	0.6	1.0	4.2	3.3	3.1	5.8	5.5	3.0
Summer	0.7	0.5	0.9	7.3	6.8	3.9	9.1	9.0	3.1
Autumn	0.8	0.4	1.0	5.3	4.7	2.9	6.5	6.0	3.4

5

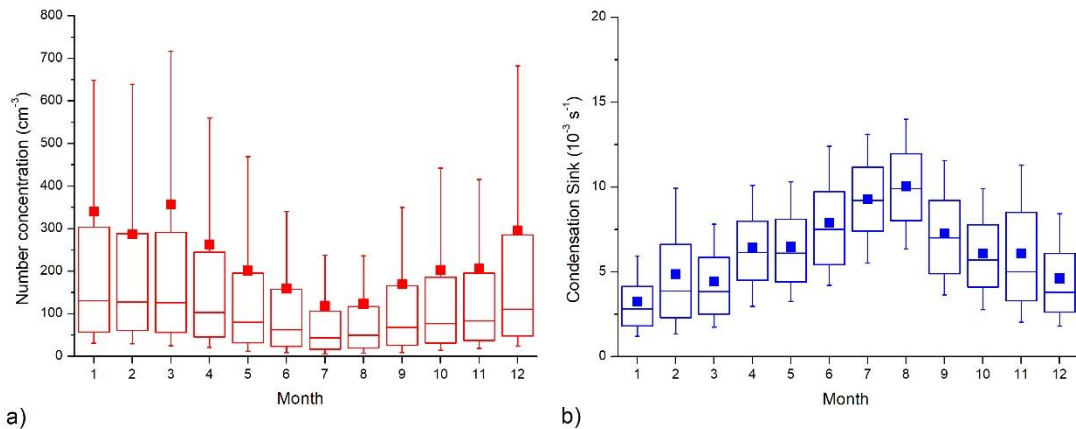
6 Table 2) Formation rates for 9nm particles (J_9), growth rates in the size range 9-25 nm (GR_{9-25})
7 for NPF events observed at Finokalia and condensational sink for sulfuric acid (CS) on seasonal
8 base during the period June 2008-June 2018 (mean, median and standard deviation).

9

10

11

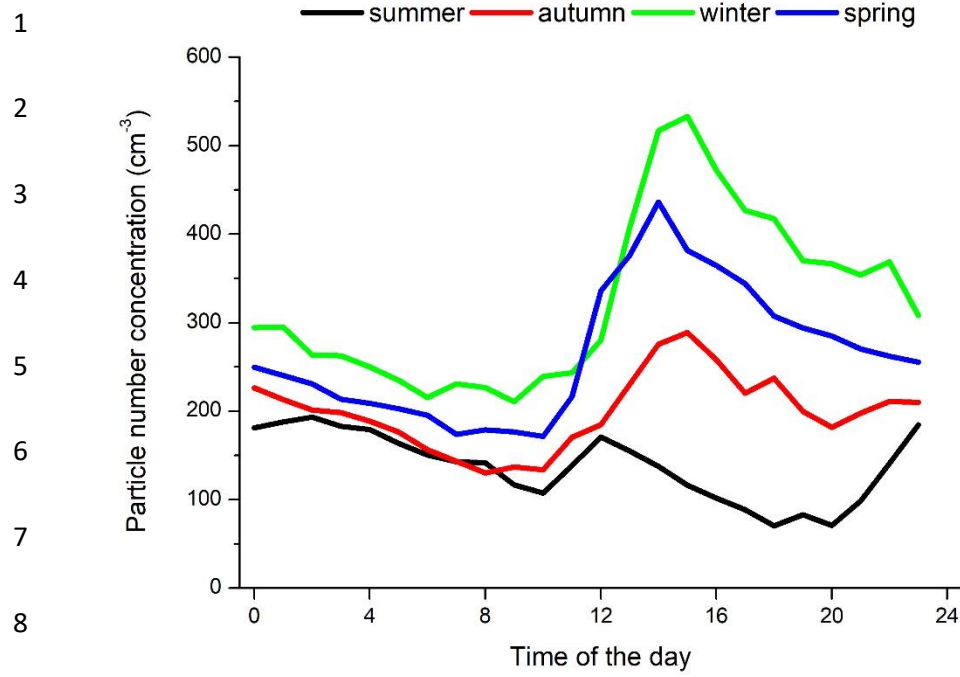
1 8) Figures



- 2 a) b)
- 3 1) Monthly average variation of a) nucleation mode particle number concentration and b)
- 4 sulfuric acid condensational sink (CS) at Finokalia station over the period June 2008-June 2018.
- 5 Whiskers represent 10th and 90th percentiles, box edges are 75th and 25th percentiles, the
- 6 line in the box is the median, the solid square is the mean.

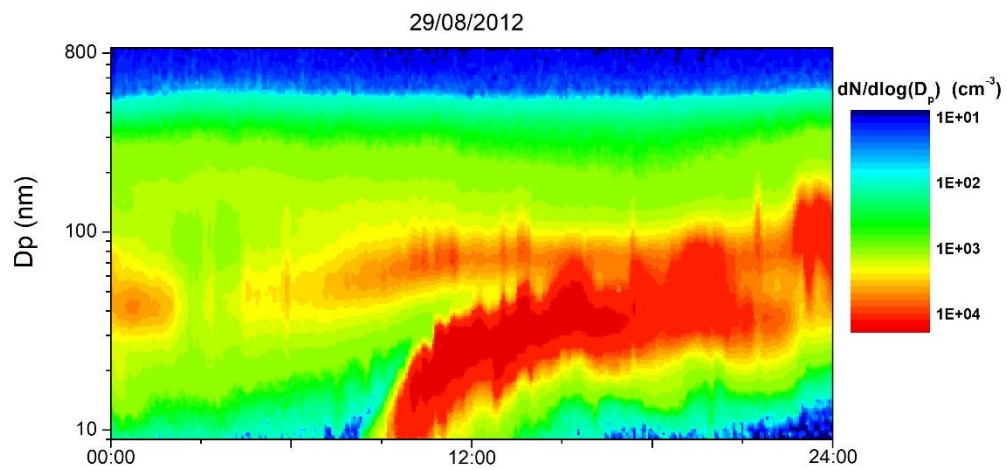
7

a)

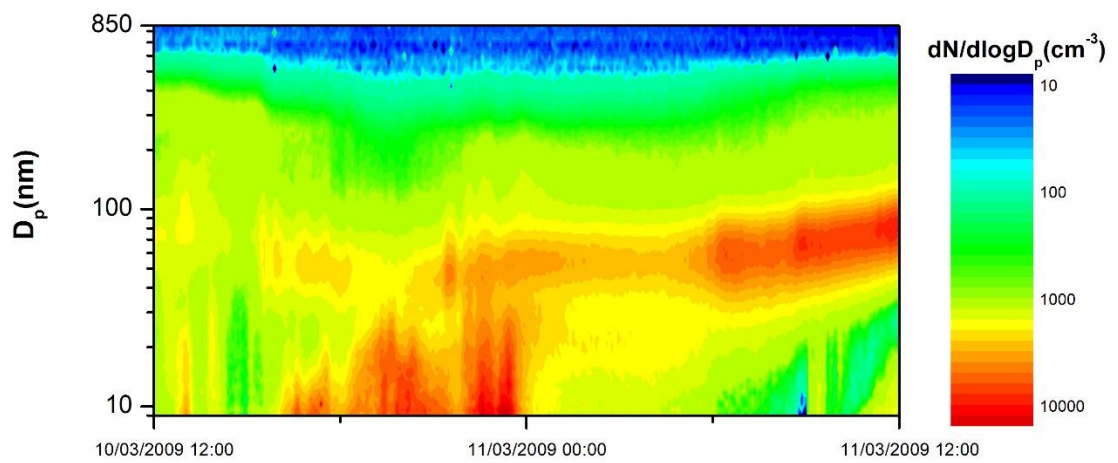


9

10 b)



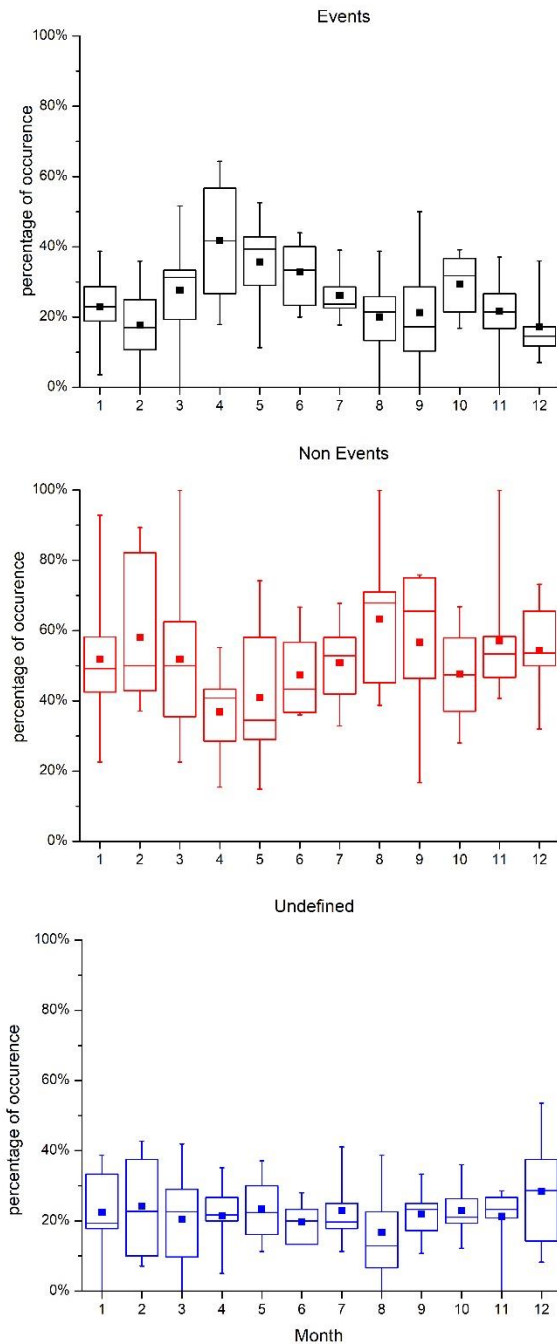
2) a) Average diurnal variation of nucleation mode particle number concentration (hourly values) at Finokalia over the period June 2008-June 2018 b) New particle formation event captured at Finokalia on 29/08/2012 (time in UTC+2).



1

2 3) Example of appearance of nucleation mode particles during several hours as observed
 3 during the night of 10 to 11/03/2009 (time in UTC+2).

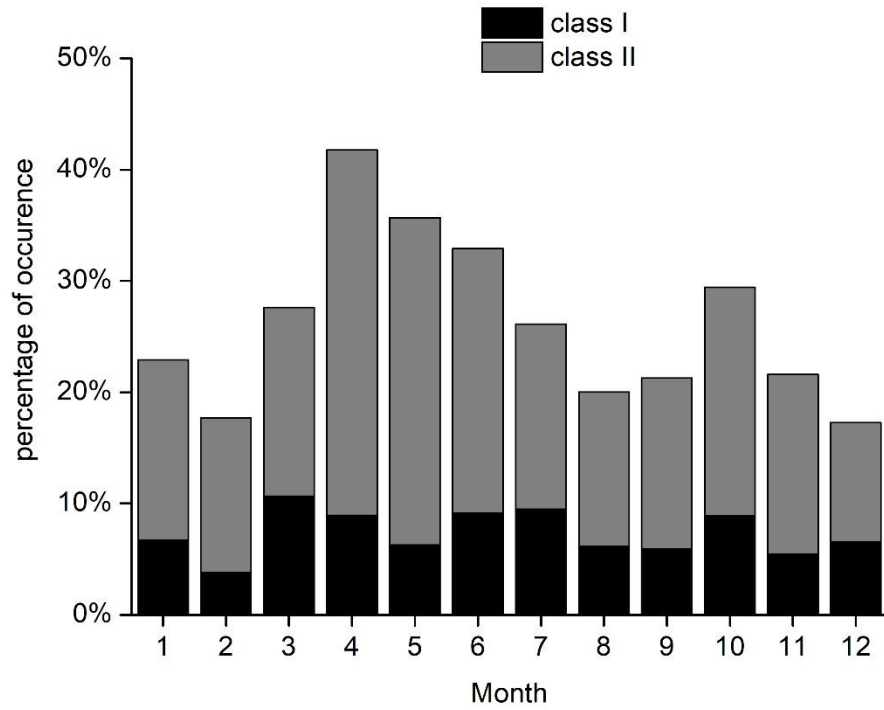
4



1

2 4) Seasonal variation of NPF percentage of occurrence of event, non-event and undefined days
3 relatively to available measurement days at Finokalia for the period June 2008-June2018.
4 Whiskers represent 10th and 90th percentiles, box edges are 75th and 25th percentiles, the
5 line in the box is the median, square is mean.

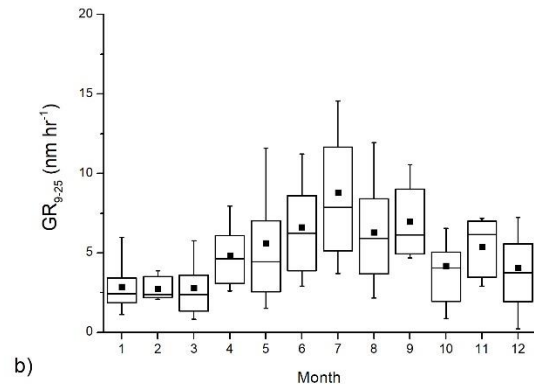
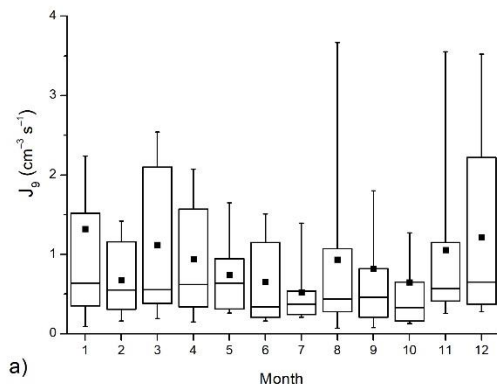
6



1

2 5) Seasonal variation of percentage of occurrence of NPF Class I & II events relatively to
 3 available measurement days at Finokalia in the eastern Mediterranean for the period June
 4 2008-June2018.

5



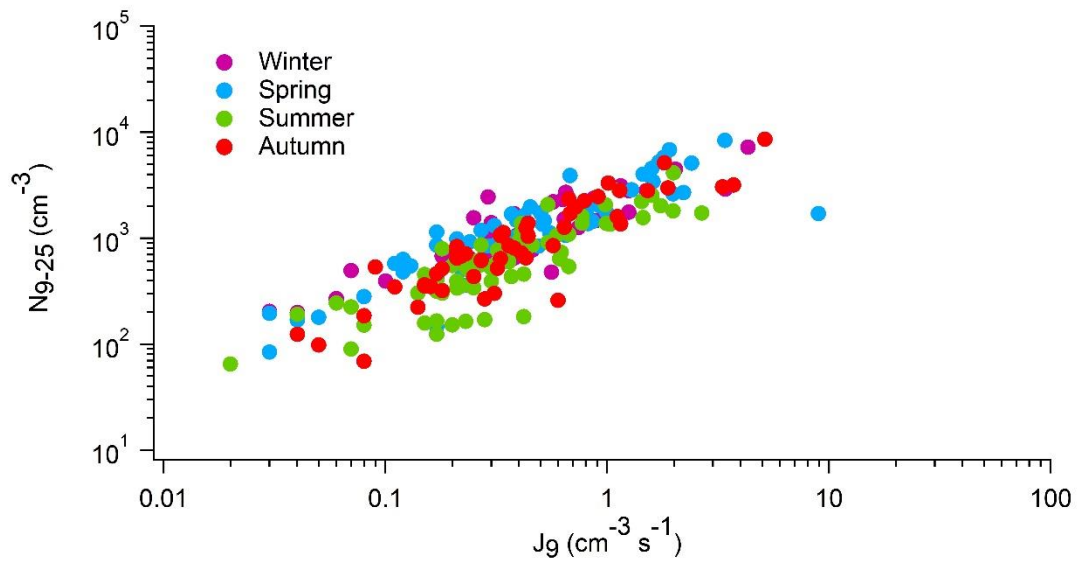
1

2

3

4 6) Seasonal variation of a) formation rate of 9nm particles (J_9) and b) growth rate in the size
5 range 9-25nm (GR_{9-25}) as calculated during Class I NPF events at Finokalia for the period June
6 2008-June 2018. Whiskers represent 10th and 90th percentiles, box edges are 75th and 25th
7 percentiles, the line in the box is the median and the solid square is the mean.

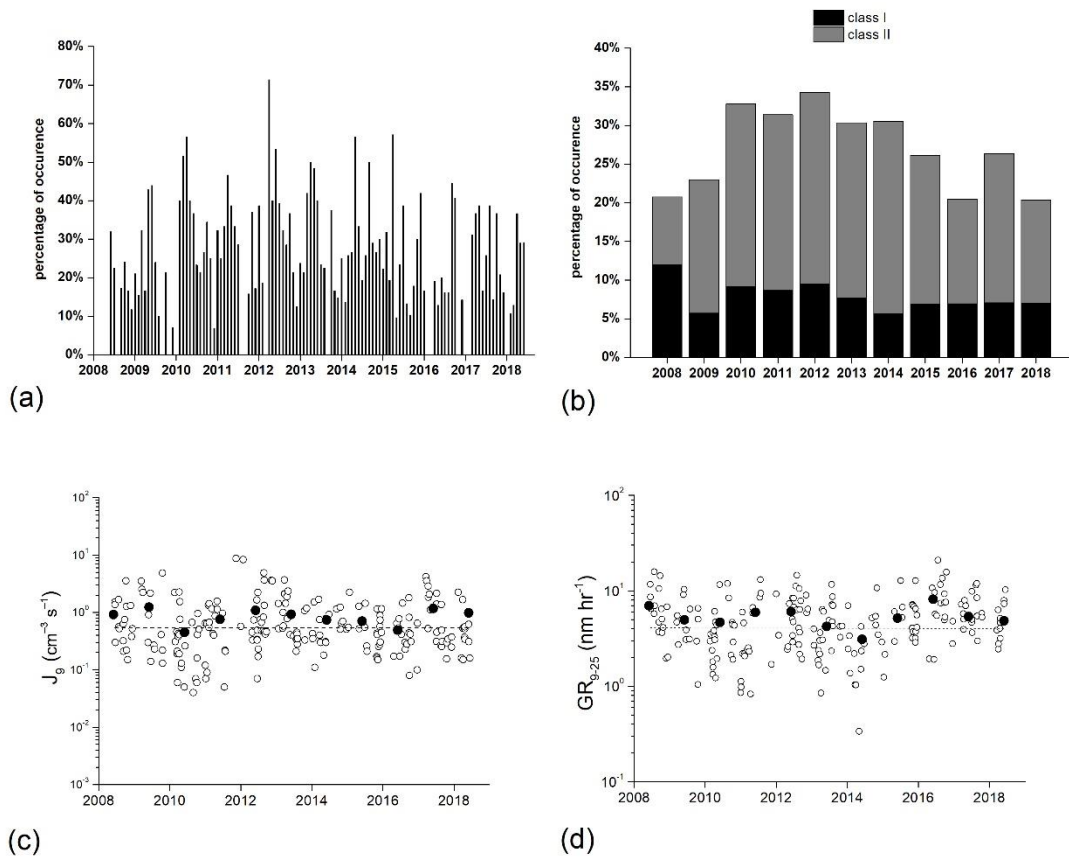
8



1

2 7) Scatter plot of formation rate of 9nm particles (J_9) versus the number concentration of
 3 nucleation mode particles (N_{9-25}) (hourly maximum value during the event) at Finokalia, for
 4 events that J_9 could be calculated with a good level of confidence (Class I events).

5



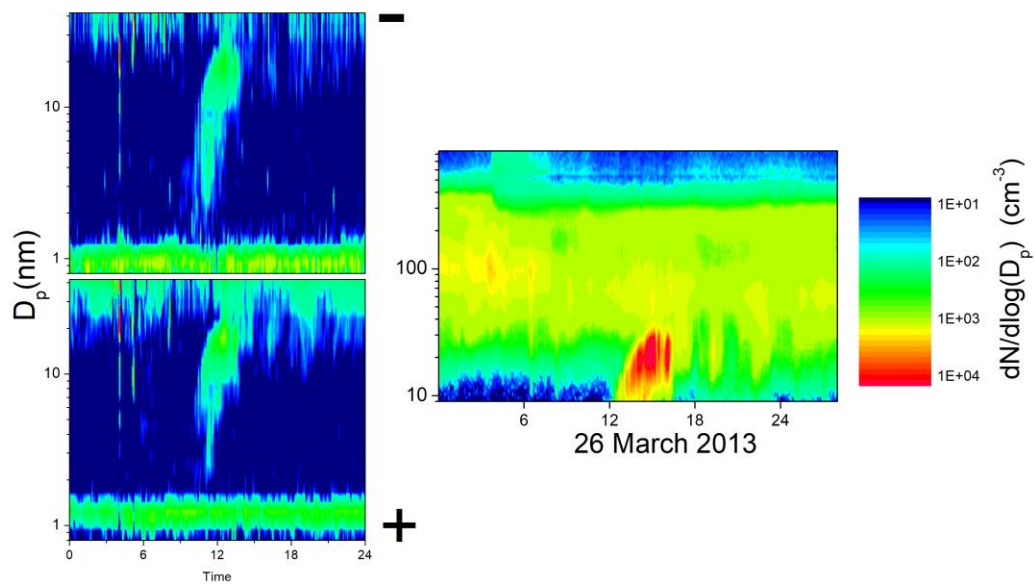
1

2 8) a) Time series of monthly NPF percentage of occurrence at Finokalia for the years 2008-
3 2018. b) Annual NPF percentage of occurrence at Finokalia for the period June 2008-June 2018
4 for Class I&II events. Interannual variation of c) formation rates of 9nm particles (J_9) and d)
5 growth rate in the size range 9-25nm (GR_{9-25}) during Class I NPF events at Finokalia for the
6 period June 2008-June 2015 (solid circles represent annual averages).

7

1

2



3

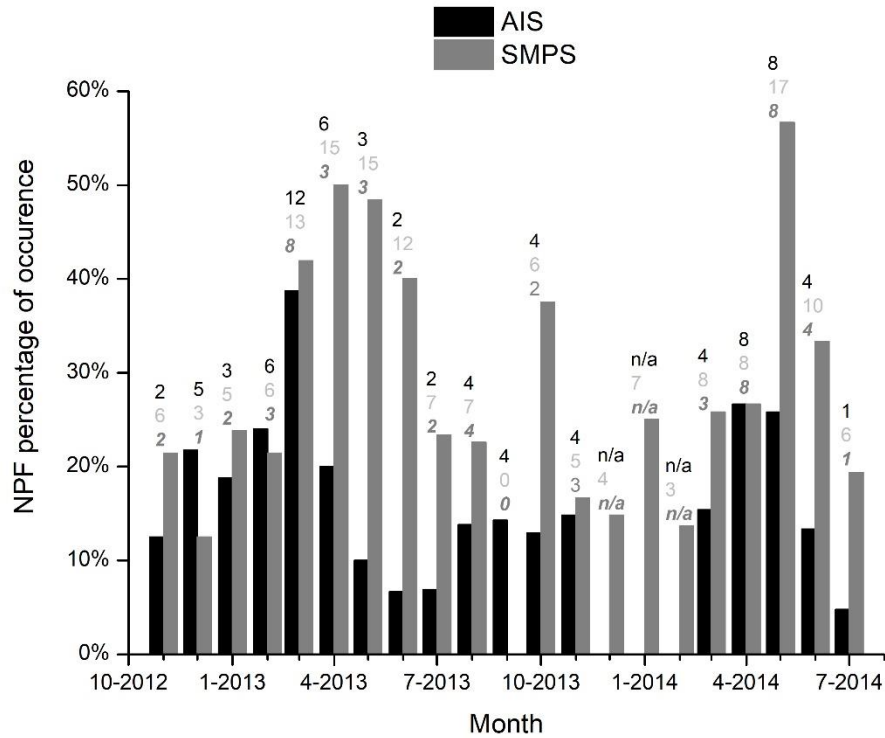
4

5

6 9) Nucleation event observed at Finokalia on 26 March 2013 as captured by AIS (left panels
 7 for negative (up) and positive (bottom) polarity) and SMPS (right panel) (time in UTC+2).

8

1

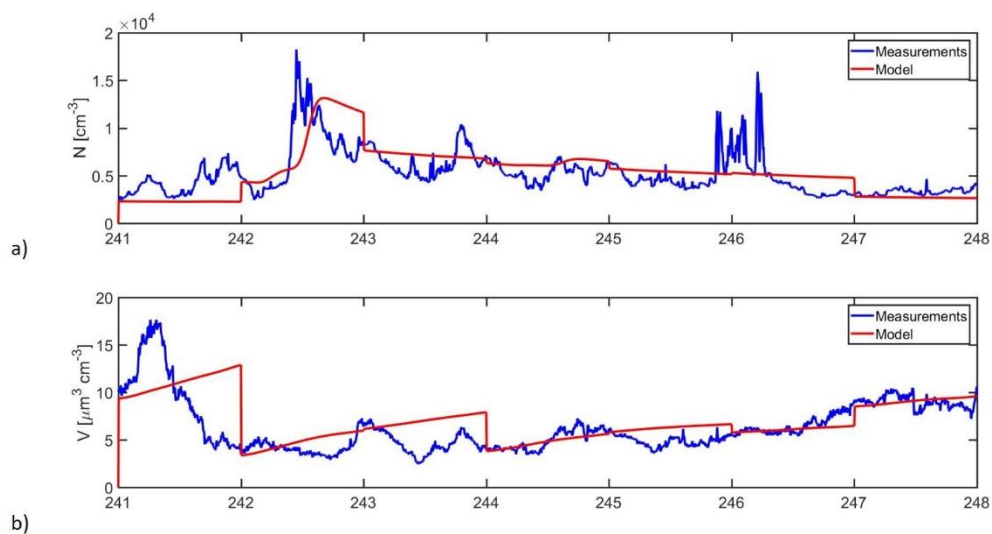


2

3 10) Monthly variability of NPF events' percentage of occurrence relatively to available
 4 measurement days at Finokalia as determined by analysis of AIS data during the FRONT
 5 experiment (Nov. 2012-July 2014). For a direct comparison, the monthly variability of NPF
 6 events as obtained from the SMPS measurements for the same period is included. On top of
 7 the columns, the NPF events observed for AIS (black), SMPS (grey) and the common events
 8 for both instruments (dark grey) for each month are presented.

9

1

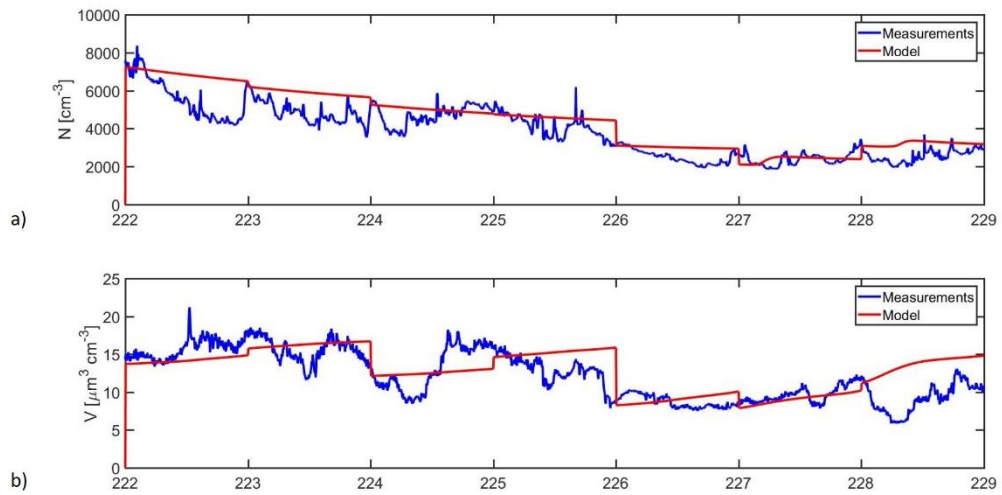


2

3

4 11) Simulations with the MALTE box with the adjusted parameters for the sub-tropical
 5 environment for the event week at Finokalia. Measured and modelled d) total number
 6 concentration and b) total volume concentration for the same period. The x-axis in both
 7 figures is Julian day of 2012.

8



1

2 12) Simulations with the MALTE box with the adjusted parameters for the sub-tropical
 3 environment for the non-event week at Finokalia. Measured and modelled d) total number
 4 concentration and b) total volume concentration for the same period. The x-axis in both
 5 figures is Julian day of 2012.

6